Interaction of Fibrin(ogen) with Leukocyte Receptor $\alpha_M\beta_2$ (Mac-1): Further Characterization and Identification of a Novel Binding Region within the Central Domain of the Fibrinogen γ-Module†

Sergiy Yakovlev,‡ Li Zhang,‡ Tatiana Ugarova,§ and Leonid Medved*,‡

University of Maryland School of Medicine, Rockville, Maryland 20855, and Joseph J. Jacobs Center for Thrombosis and Vascular Biology, Cleveland, Ohio 44195

Received August 11, 2004; Revised Manuscript Received September 30, 2004

ABSTRACT: The fibrinogen γ-module sequences, γ190−202 or P1, and γ377−395 or P2, were implicated in interaction with the α_MI-domain of the leukocyte receptor $\alpha_M\beta_2$. P1 is an integral part of the γ-module central domain, while P2 is inserted into this domain forming an antiparallel β-strand with P1. We hypothesized earlier that separation of P2 from P1 may regulate interaction of fibrin(ogen) with leukocytes during the inflammatory response. To test the relative contributions of these sequences to the interaction and the effect of their separation, we prepared the recombinant γ-module (γ148−411) and its halves, γ148−286 and γ287−411 fragments containing P1 and P2, respectively, and evaluated their affinities for the recombinant α_MI-domain. In a solid-phase binding assay, the immobilized γ-module exhibited high affinity for α_MI (K_d = 22 nM), while the affinities of the isolated γ148−286 and γ287−411 halves were much lower (K_d's = 521 and 194 nM, respectively), indicating that both halves contribute to the interaction in a synergistic manner. This is consistent with the above hypothesis. Further, we prepared the recombinant γ148−191 and γ192−286 fragments corresponding to the NH_2-terminal and central domains, respectively, as well as γ148−226 containing P1, and tested their interaction with α_MI. The immobilized γ192−286 fragment bound to α_MI with K_d = 559 nM, while both γ148−191 and γ148−226 failed to bind suggesting that P1 does not contribute substantially to the binding and that the binding occurs mainly through the γ227−286 region. To further localize a putative binding sequence, we cleaved γ192−286 and analyzed the resulting peptides. The only α_MI-binding activity was associated with the γ228−253 peptide, indicating that this region of the central domain contains a novel $\alpha_M\beta_2$-binding sequence.

Interaction between fibrin(ogen) and leukocyte integrin $\alpha_M\beta_2$, or Mac-1, plays an important role in the attraction of inflammatory cells to places of injury during normal wound healing as well as to places of chronic inflammation in which fibrin(ogen) is present. Numerous studies performed to establish the mechanism of this interaction revealed that it occurs primarily through the I-domain of the integrin α_M subunit, α_MI,[1] and the terminal D regions of fibrin(ogen). Particularly, it was found that a proteolytically prepared 30-kDa fragment derived from the fibrinogen D region inhibited binding of fibrinogen to stimulated monocytes and neutrophils (*1*) and that a recombinant γ-module including γ chain residues 148−411 of this region supported adhesion of $\alpha_M\beta_2$-transfected cells (*2*). Further, studies with synthetic peptides suggested that two sequences within the γ-module, γ190−202 and γ373−395, designated as P1 and P2, respectively, are involved in the $\alpha_M\beta_2$ recognition (*3*, *4*). It was also shown that deletion of the α_MI domain from $\alpha_M\beta_2$ completely abrogated the binding of $\alpha_M\beta_2$ to fibrinogen (*5*).

Among the two peptides, P2 was found to be the more potent inhibitor of adhesion of the $\alpha_M\beta_2$-expressing cells (*4*). This together with the subsequent finding that deletion of the P2 sequence in the γ-module reduced its binding to the α_MI-domain while mutation of several residues in P1 had no effect lead to the conclusion that the P2 sequence is the major binding site for $\alpha_M\beta_2$ (*6*). In addition, a minimal recognition motif within P2 was localized to the residues γ390−395 (*6*). At the same time, experiments with recombinant fibrinogen mutants devoid of this motif suggested that deletion of these residues in the context of the whole molecule is not sufficient to ablate function (*6*). In fact, such mutants were as effective in supporting adhesion of $\alpha_M\beta_2$-expressing cells as the wild type and plasma fibrinogens (*6*), suggesting that the structural basis for the interaction between fibrinogen and $\alpha_M\beta_2$ could be more complex. In addition, the fact that these sites are cryptic in fibrinogen and become unmasked only when it is immobilized onto plastic or deposited in the extracellular matrix (*7*) further adds to the

† This work was supported by National Institute of Health Grant HL-56051 to L.M., HL-61589 to L.Z, and HL-63199 to T.U.

* To whom correspondence should be addressed at University of Maryland School of Medicine, 15601 Crabbs Branch Way, Rockville, MD 20855. Tel: 301-738-0719. Fax: 301-738-0740. E-mail: medvedL@usa.redcross.org.

‡ University of Maryland School of Medicine.

§ Joseph J. Jacobs Center for Thrombosis and Vascular Biology.

[1] Abbreviations: α_MI-domain, a region of ~200 amino acid residues "inserted" in the α_M subunit of integrin $\alpha_M\beta_2$; γ-module, COOH-terminal region of the fibrinogen γ chain including residues 148−411; P1 and P2, the fibrinogen γ-module sequences including residues γ190−202 and γ377−395, respectively; GST, glutathione *S*-transferase; TBS, 20 mM Tris buffer, pH 7.4, with 0.15 M NaCl; PVDF membtane, poly(vinylidene difluoride) membrane; HEK 293 cells, human embryonic kidney cells; SPR, surface plasmon resonance.

10.1021/bi048266w CCC: $30.25
Published on Web 12/13/2004

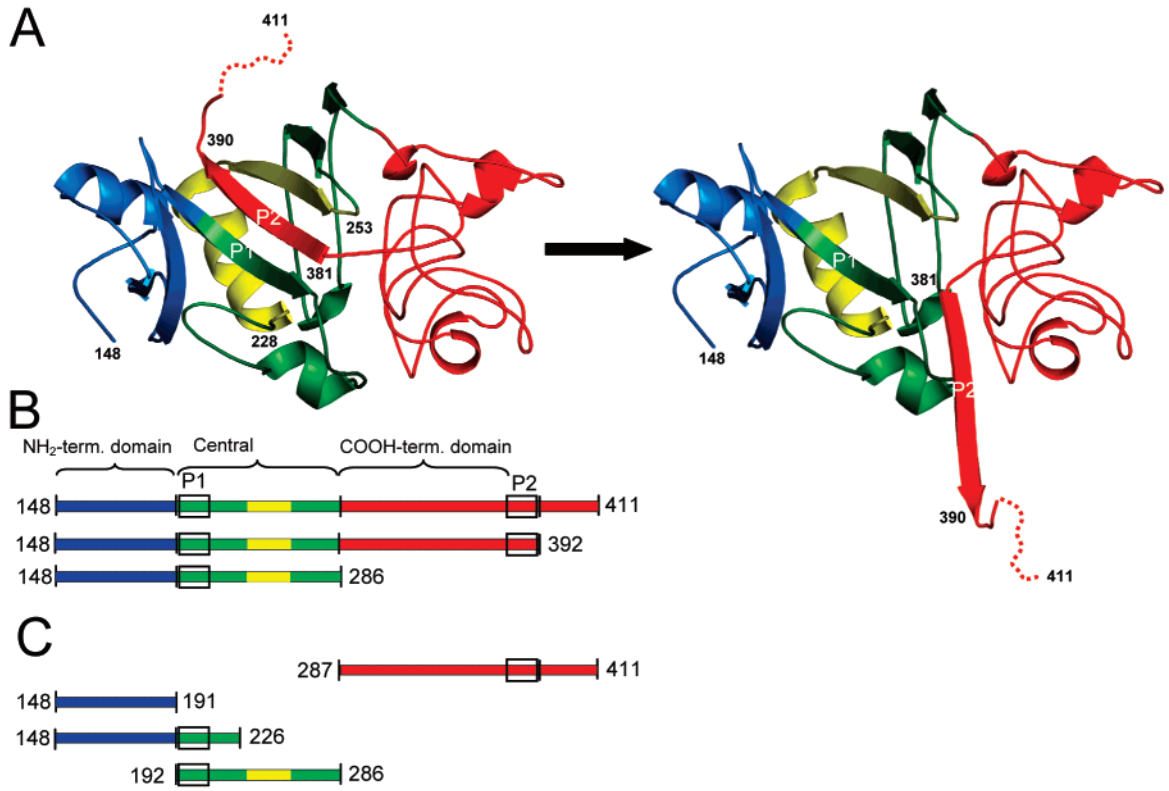

FIGURE 1: Schematic representation of the recombinant γ-module and its truncated variants expressed for this study. The ribbon diagram of the γ-module (residues γ148−411) based upon its crystal structure (PDB ID 1FIB; ref 8) is presented in panel A at the left. A hypothetical structure of the γ-module in which the γ381−390 β-strand insert was pulled-out from the central domain using molecular modeling with the program DS ViewerPro (Accelrys, San Diego, CA) is presented in panel A at the right. Both diagrams were constructed using the program PyMol (DeLano Scientific, San Francisco, CA). The NH_2-terminal domain (residues γ148−191) is colored in blue, the central domain (residues 192−286) is in green and yellow, and the COOH-terminal portion of the γ-module is in red. The γ228−253 region of the central domain is colored in yellow (see text). The extreme COOH-terminus (residues 393−411) whose position was not determined in the crystal structure (*8*) is presented by a dotted curved line. Panel B represents schematically the γ-module and its truncated variants, γ148−286 and γ148−392, expressed earlier (*2*, *9*). The γ-module variants, γ287−411, γ148−191, γ148−226, and γ192−286, expressed in this study are represented in panel C. The color scheme in panels B and C follows the same pattern as in panel A. The approximate location of P1 and P2 including residues γ190−202 and γ377−395, respectively (*3*, *4*), are shown by open boxes.

complexity of this interaction. Thus, despite substantial progress in our understanding of the fibrin(ogen)−$\alpha_M\beta_2$ interaction, the structure of the $\alpha_M\beta_2$-binding site and the mechanism of its interaction still need to be further clarified.

The crystal structure of the fibrinogen γ-module (*8*) revealed that it consists of three independently folded domains formed by residues γ148−191, γ192−286, and γ286−380, respectively, and that its COOH-terminal residues γ381−390 including part of P2 are inserted into the central domain (γ192−286), while the rest (γ393−411) seems to be flexible (Figure 1A, left diagram). Since with such arrangement both P1 and P2 sequences reside in close proximity forming two antiparallel β strands in the central domain (*8*), it was suggested that their juxtaposition may form a complex binding site for $\alpha_M\beta_2$ (*4*). Our denaturation study revealed that although the γ381−390 β-strand insert contributes to the stability of the central domain, it can be removed without destroying the compact structure of the latter (*9*). On the basis of this and some other observations, we hypothesized that the β-strand insert may be removed (pulled out) from the γ-module (Figure 1A, right diagram) and that such a "pull out" mechanism could be functionally relevant (*9*, *10*). Particularly, we hypothesized that P1 and P2 could be separated by this mechanism and that such separation could alter the $\alpha_M\beta_2$-binding activity of the γ-module, thus modulating fibrinogen−leukocyte interaction during an inflammatory response (*9*).

In this study, we prepared the recombinant individual domains of the γ-module and combinations thereof containing the P1 or P2 sequences, as well as the recombinant α_MI-domain, and tested the effect of separation of these sequences on the $\alpha_M\beta_2$-binding activity. The experiments revealed that although the individual P1- and P2-containing domains could interact with α_MI independently, they should act together for high affinity binding to occur. We also found that the central domain of the γ-module contains a novel $\alpha_M\beta_2$-binding sequence which was further localized within its γ228−253 region.

EXPERIMENTAL PROCEDURES

Expression of the Recombinant γ-Module and Its Variants. The recombinant wild type γ-module corresponding to the human fibrinogen γ chain residues 148−411 and its truncated variants, γ148−392 and γ148−286 (Figure 1B), were produced in *Escherichia coli* using a pET-20b expression vector, purified, and refolded as described earlier (*2*, *9*). This vector was used as a template to produce several new truncated variants of the γ-module, γ287−411, γ148−191, γ148−226, and γ192−286 (Figure 1C). A cDNA encoding γ148−191, γ148−226, and γ287−411 variants was pro-

duced by polymerase chain reaction (PCR) using the following primers in which the restrictase−recognition sequences are underlined here and elsewhere,

5′-TTTCCCTCTAGAAATAATTTTGTTTAACTTTAAG-3′ (forward) and

5′-TTTAAAAAGCTTTCACCATCCATTTCCAGACCCATCG-3′ (reverse) for γ148−191,

5′-TGGAAATCATATGATCACTGGGAAAGATTGTCAAG-3′ (forward) and

5′-TTTAAAAAGCTTTCAAAATTCTGTTGTGCCAGTAG-3′ (reverse) for γ148−226,

5′-TGGAAATCATATGGGAGATGCCTTTGATGGCTTTG-3′ (forward) and

5′-TTTAAAAAGCTTTCAAACGTCTCCAGCCTGTTTG-3′ (reverse) for γ287−411.

The PCR products were subcloned into the pET-20b expression vector (Novagen) using *Nde*I and *Hind*III restriction sites for γ148−226 and γ287−411, and *Xba*I and *Hind*III restriction sites for γ148−191, and then transformed into DH5α *E. coli* host cells (Invitrogen). To produce a cDNA encoding γ192−286, we used forward primer

5′-TGGAAATCATATGACTGTGTTTCAGAAGAGACTTG-3′ and two reverse primers,

5′-TGGGATGGCAGACTGTGTG-3′ and

5′-TTTAAAAAGCTTTCAAGCATCCCCACCAGCGAAG-3′. Since the resulting two PCR products contained an *Apo*I restriction site, both PSR products were subcloned into the pET-20b expression vector (Novagen) using *Nde*I, *Apo*I, and *Hind*III restriction sites. All resultant clones were sequenced to confirm the integrity of the coding sequences.

For production of protein fragments, the BL21/pLysS *E. coli* host cells were transformed with the resulting plasmids, and all variants of the γ-module were purified and refolded following the procedures described previously for the recombinant wild-type γ-module (*2*, *9*). The purity of the resulting γ-module variants was verified by SDS−PAGE and by NH_2-terminal sequence analysis. The sequence analysis was performed with a Hewlett-Packard model G 1000S sequencer. The NH_2-termini of the fragments were determined by direct sequencing for six cycles.

Expression and Purification of the Recombinant α_MI-Domain. The recombinant α_MI-domain was expressed as glutathione *S*-transferase (GST) fusion proteins in *E. coli* as described previously (*11*) and purified from the soluble fractions of bacterial lysates by affinity chromatography using glutothion-Sepharose (Amersham Biosciences). The coding region for the α_MI-domain (residues Glu^{123}−Lys^{315}), in which Cys^{128} was changed to Ser (*12*), was amplified by polymerase chain reactions using plasmid pCIS2M-hCD11b as a template (*11*), which contain the cDNA fragments coding for the full-length α_M subunit of integrin $\alpha_M\beta_2$. The primers used for the α_MI-domain were 5′AATTGGATCCTTGAGGCCCTCAGAGGTTCTCCCCAAGAGGATAGTGTACATTGCC3′ (forward) and 5′ATTCTCGAGTTACTTCTCCCGAAGCTGGTTCTG3′ (reverse). The PCR product was subcloned into the pGEX-5X-3 expression vector (Amersham Biosciences) using *BamH*I and *Xho*I restriction sites. The resultant clone was sequenced to confirm the integrity of the coding sequence. The plasmid was transformed in *E. coli* strain BL-21(DE3)pLysS competent cells, and expression was induced by the addition of 1 mM isopropyl-1-thio-β-D-galactopyranoside for 3−5 h at 37 °C. To cleave the α_MI-domain from the GST-fusion part, 1 mg of GST-α_MI-domain in 20 mM Tris, pH 7.4, 0.15 M NaCl (TBS) containing 2 mM $CaCl_2$ was incubated with 20 μg of factor Xa (New England Biolabs) overnight at room temperature. Benzamidine-agarose (Sigma) was used to isolated Factor Xa from the reaction mixture. The α_MI-domain was further separated from GST and noncleaved GST-α_MI-domain by affinity chromatography on glutathione-sepharose (Amersham Biosciences). The α_MI-domain was biotinilated with EZ-Link NHS−Biotin (Pierce) as recommended by the manufacturer.

Chemical Fragmentation of γ192−286. The recombinant fibrinogen γ192−286 fragment, corresponding to a central domain of the γ-module, was cleaved by *o*-iodosobenzoic acid in the presence of *p*-cresol as described in ref *13*. Briefly, 200 μL of the fragment at 10 mg/mL in 4 M GdmCl was mixed with 800 μL of acetic acid followed addition 2 mg of *o*-iodosobenzoic acid. The cleavage was performed overnight at room temperature in the presence of 3 μL of *p*-cresol. Under these conditions, *o*-iodosobenzoic acid selectively cleaves proteins at tryptophan residues (*13*). Resulting peptides were separated by high-performance liquid chromatography (HPLC) on a reverse-phase C18 Vydac column. The column was equilibrated with 0.1% trifluoroacetic acid in water and eluted with a gradient of 0.1% trifluoroacetic acid in acetonitrile. The flow rate was 1.0 mL/min.

Protein Concentration Determination. Concentrations of the recombinant fragments were determined spectrophotometrically using extinction coefficients ($E_{280,1\%}$) calculated from the amino acid composition by the following equation: $E_{280,1\%} = (5690W + 1280Y + 120S-S)/(0.1M)$, where W, Y, and S−S represent the number of Trp and Tyr residues and disulfide bonds, respectively, and M represents molecular mass (*14*). Molecular masses of the recombinant fragments were calculated based on their amino acid composition. The following values of molecular masses and $E_{280,1\%}$ were obtained for the newly expressed fragments: γ148−191, 5.0 kDa and 16.9; γ148−226, 9.0 kDa and 17.1; γ192−286, 10.9 kDa and 22.6; γ287−411, 14 kDa and 29.0; α_MI-domain, 22 kDa and 1.74. Concentrations of the previously described fragments, γ148−411, γ148−392, and γ148−286, were determined as in ref *9*.

Fluorescence Study. Fluorescence spectra were recorded in an SLM 8000-C fluorometer. Fluorescence measurements of thermal unfolding were performed by monitoring the ratio of the intensity at 350 nm to that at 320 nm with excitation at 280 nm in the same fluorometer. Temperature was controlled with a circulating water bath programmed to raise the temperature at 1 °C/min. Protein concentrations were 0.02−0.03 mg/mL. All experiments were performed in 20 mM Tris, pH 8.0.

Cell Adhesion Assay. Adhesion assays with HEK 293 cells expressing $\alpha_M\beta_2$ (*15*) were performed essentially as described in ref *16*. Briefly, the $\alpha_M\beta_2$-expressing cells grown in DMEM/F-12 supplemented with 25 mM HEPES and 10% fetal bovine serum were labeled with Calcein AM (Molecular Probes, Eugene, OR) and resuspended in HBSS (Hank's balanced salt solution) at 2.5×10^5 cells/mL. The labeled cells (100 μL aliquots) were added to the wells coated with 5 μg/mL the γ-module or its fragments, and post-coated with 1% PVP (poly(vinylpyrrolidone)). After 30 min incubation at 37 °C in 3% CO_2, the nonadherent cells were removed

and the fluorescence was measured in a fluorescence plate reader (Applied Biosystems, Farmington, MA).

Ligand Blotting Assay. The recombinant γ-module variants were subjected to SDS electrophoresis using NuPAGE Bis-Tris electrophoretic system (Invitrogen), and then electrotransferred to a poly(vinylidene difluoride) (PVDF) membrane (Invitrogen). To check the effectiveness of protein transfer, the membrane was stained with MemCode reversible protein stain kit for PVDF membrane (Pierce). The membrane then was blocked for 1 h at room temperature with WesternBreeze Blocker/Diluent (Invitrogen) solution as recommended by manufacturer followed by overnight incubation at 4 °C with 10 μg/mL biotinylated recombinant α_MI-domain in the antibody diluent, which was prepared as described in the instruction manual for WesternBreeze Chemiluminescent Western Blot Immunodetection kit (Invitrogen). Bound α_MI domain was detected via its biotin moiety by reaction with streptavidin conjugated to alkaline phosphatase (Sigma) diluted 1:50000 with the same antibody diluent and visualized by using chemiluminescent substrate CDP-Star from Tropix (Bedford, MA) according to the manufacturer recommendations. WesternBreeze wash solution (Invitrogen) was used to wash the membrane from the biotinylaned α_MI-domain and from streptavidin conjugated to alkaline phosphatase.

Solid-Phase Binding Assay. Wells of high-binding microplates (Fisher) were coated overnight at 4 °C with 100 μL/well of 2 μg/mL γ-module variants at 0.1 M Na_2CO_3, pH 9.5 (coating buffer). The wells were then blocked with SuperBlock blocking buffer in TBS (Pierce) for 2 h at room temperature. Following washing of the sample with TBS containing 0.05% Tween 20 (TBS-T), the indicated concentrations of the biotinylated recombinant α_MI-domain in TBS-T containing 1 mM $MnCl_2$ were added to the wells and also to control wells coated with just SuperBlock blocking buffer and incubated overnight at 4 °C. The binding of the α_MI-domain was measured by the reaction with streptavidin conjugated to alkaline phosphatase. The alkaline phosphatase substrate, *p*-nitrophenyl phosphate (Pierce), was added to the wells and the amount of bound ligand was measured after 20 min spectrophotometrically at 405 nm. Data were fitted by nonlinear regression analysis using eq 1:

$$B = B_{max}/(1 + K_d/[L])$$

where B represents the amount of ligand bound, B_{max} is the concentration of ligand bound at saturation (or the signal proportional to it), [L] is a molar concentration of free ligand, assumed here to be equal to total, and K_d is the dissociation constant.

Surface Plasmon Resonance. The interaction of the α_MI-domain with the γ-module and its variants, γ148−286 and γ287−411, was studied by surface plasmon resonance using the BIAcore 3000 biosensor (Biacore AB, Uppsala, Sweden), which measures association/dissociation of proteins in real time. The γ-module variants were immobilized to the CM5 sensor chip using the amine coupling kit (BIAcore AB, Uppsala, Sweden) according to the manufacturer instructions. The γ148−411 was immobilized at 50 μg/mL in 10 mM sodium acetate, pH 5.0; for immobilization of the γ148−286 and γ287−411 fragments, 100 mM sodium acetate, pH 4.0, was used. Biosensor surfaces were coupled to final response values of ~1000 response units (RU).

Binding experiments were performed in HBS-P buffer (BIAcore AB, Uppsala, Sweden) containing 1 mM $MnCl_2$ at 10 μL/min flow rate. The α_MI-domain was injected at different concentrations and the association between immobilized γ-module fragments and the added α_MI-domain was monitored as the change in the SPR response; the dissociation was measured upon replacement of the ligand solution for the buffer without ligand. To regenerate the chip surface, complete dissociation of the complex was achieved by adding a solution containing 20 mM NaOH and 1 M NaCl for 1 min followed reequilibration with the binding buffer. Experimental data were analyzed using BIAevaluation 3.2 software supplied with the instrument.

RESULTS

Expression and Characterization of the γ-Module Variants. We had previously expressed in *E. coli* the full-length γ-module (residues γ148−411) and its fragments, γ148−392 devoid of the flexible COOH-terminal portion, and γ148−286 including the NH_2-terminal and central domains (residues γ148−191 and γ192−286, respectively) (*2*, *9*) (Figure 1B). Denaturation experiments revealed that all three species were folded into a compact structure (*2*, *9*). For this study, we prepared the γ-module and both above-mentioned fragments, as well as four new fragments. They include the γ148−191 and γ192−286 fragments corresponding to the NH_2-terminal and central domains, respectively, γ287−411 containing the COOH-terminal domain and an extra 381−411 portion with P2, and γ148−226 including the NH_2-terminal domain and an extra portion with P1 (Figure 1C). Before refolding, the γ287−411 and γ192−286 fragments exhibited fluorescence spectra with maximum at 352 nM, which shifted after refolding to 345 and 347 nm, respectively (insets in Figure 2 A,B). This is consistent with the presence of a compact structure in both fragments. Moreover, when the samples were heated in the fluorometer while the ratio of fluorescence intensity was monitored at 350 nm to that at 320 nm as a measure of the spectral shift that accompanies unfolding, γ287−411 exhibited a sigmoidal denaturation transition with a midpoint at 51 °C (Figure 2A), close to that observed earlier with the full length γ-module (*2*). This indicates that the COOH-terminal domain composing most of the γ287−411 fragment was folded and stable. The other fragment, γ192−286, exhibited aggregation upon denaturation resulting in a downward change in fluorescence ratio, which started at about 45 °C (Figure 2B). This indicates that the recombinant central domain was also folded and stable.

It should be noted that the γ148−286 and γ287−411 fragments each represented about half of the γ-module, and that the former contained the P1 sequence while the latter contained P2. Since our data indicate that both fragments were folded into a stable compact structure, it is likely that the overall conformation of each fragment was similar to that expected for the intact γ-module, with its P2 β-strand removed from the central domain (Figure 1A, right diagram). These fragments together with the γ-module and its truncated variant, γ148−392, were used to evaluate the relative contribution of the P1 and P2 sequences to the interaction with $\alpha_M\beta_2$.

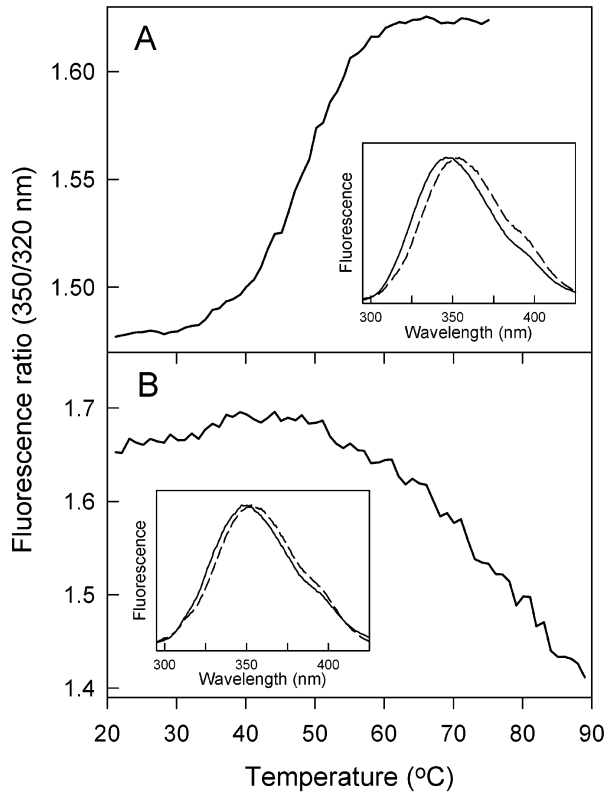

FIGURE 2: Fluorescence-detected thermal denaturation of the recombinant fragments. Panels A and B show melting curves of the recombinant γ287−411 and γ192−286 fragments, respectively, obtained upon their heating in 20 mM Tris, pH 8.0. The insets in both panels show the fluorescence spectra of the corresponding fragments at 20 °C after refolding (solid lines) and in 4 M GdmCl before refolding (dashed lines).

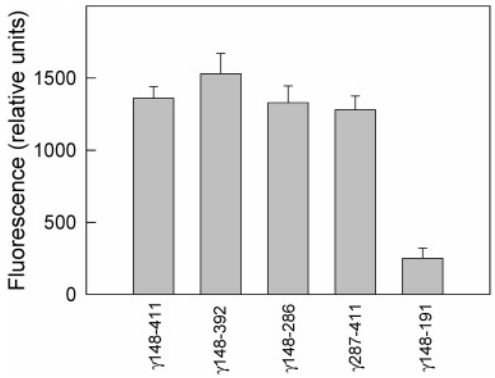

FIGURE 3: Adhesion of $\alpha_M\beta_2$-expressing cells to the recombinant γ-module and its truncated variants. Aliquots of $\alpha_M\beta_2$-transfected cells labeled with Calcein AM (2.5×10^4 cells/0.1 mL) were incubated with the microtiter wells coated with 5 μg/mL the γ-module and its fragments, γ148−191, γ148−286, γ148−392, and γ287−411, and post-coated with 1% PVP. After 30 min at 37 °C, nonadherent cells were removed by three washes with PBS. Results are expressed as fluorescence of adherent cells and are the mean ± SD values from three individual experiments.

Cell Binding Study. In adhesion assays, wells were coated with the recombinant γ-module and its variants, followed by incubation with fluorescence-labeled $\alpha_M\beta_2$-expressing cells. These cells adhered well to the γ-module and its truncated variant γ148−392, and to its NH_2- and COOH-terminal halves, γ148−286 and γ287−411 containing P1 and P2, respectively (Figure 3). The adhesion to the γ148−191 fragment corresponding to the NH_2-terminal domain of

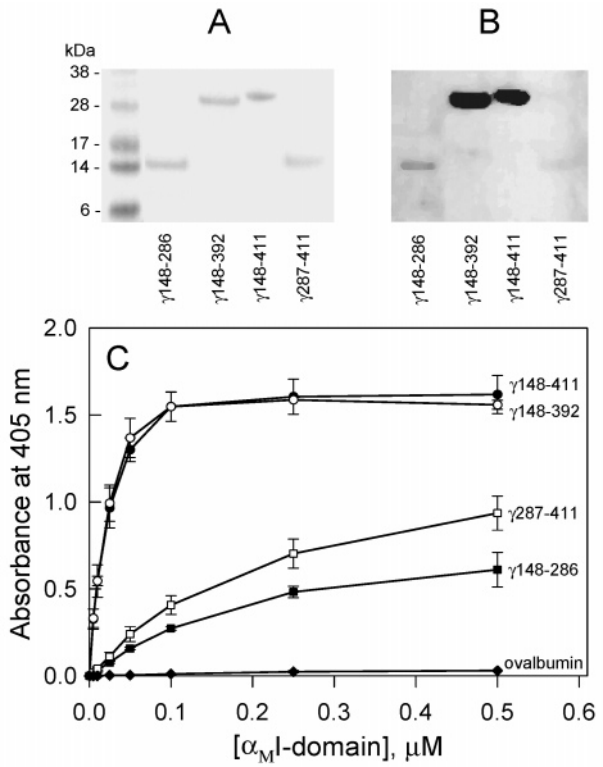

FIGURE 4: Analysis of binding of the α_MI-domain to the recombinant γ-module and its truncated variants by ligand blotting and solid-phase binding assay. The indicated recombinant fragments, γ148−286, γ148−392, γ148−411, and γ287−411, were transferred to the PVDF membrane after SDS−PAGE, stained with MemCode reversible protein stain kit (Pierce) (panel A), and then probed with biotinylated α_MI-domain after destaining (panel B). Panel C shows the results of the solid-phase binding assay. Increasing concentrations of the biotinylated α_MI-domain were incubated with microtiter wells coated with the indicated fragments and ovalbumin, which was used as a control. Bound α_MI-domain was detected using streptavidin conjugated to alkaline phosphatase. Error bars reflect the standard deviation of three independent determinations. All experiments were performed in TBS containing 1 mM $MnCl_2$. Solid lines represent best fits of the data to eq 1, and the corresponding values of K_d are presented in Table 1.

the γ-module was much lower but still noticeable. Although this adhesion presumably occurred through the interaction with $\alpha_M\beta$ integrin, one could not exclude contribution of some other unidentified $\alpha_M\beta_2$-independent mechanism(s). Therefore, to further characterize binding of these fragments to $\alpha_M\beta_2$, we studied their interaction with the recombinant α_MI-domain of $\alpha_M\beta_2$ by various techniques.

Interaction between the α_MI-Domain and the γ-Module Variants Detected by Ligand Blotting. In ligand blotting experiments, the γ-module and its fragments were transferred to a PVDF membrane after SDS−PAGE and probed with the biotinylated α_MI-domain (Figure 4 A,B). The experiments revealed that α_MI exhibited strong binding to the γ-module and its truncated γ148−392 fragment, and weak binding to its NH_2- and COOH-terminal halves, γ148−286 and γ287−411. These indicate that the isolated halves interact with the α_MI-domain; however, the interaction is much stronger when they are combined in the γ-module. To obtain quantitative information about the relative contribution of the P1 and P2 sequences to the interaction of the γ-module with α_MI, we turned to a solid-phase binding assay.

Table 1: Dissociation Constants (K_d) for the Interaction of the α_MI-Domain with the Recombinant γ-Module and Its Variants Obtained by Solid Phase Binding Assay and Surface Plasmon Resonance

fragments	K_d (SPB)[a] (nM)	K_d (SPR)[b] (μM)
γ148−411	22 ± 1	5.5 ± 0.2
γ148−392	21 ± 2	
γ148−286	521 ± 10	17.6 ± 3.1
γ287−411	194 ± 8	11.7 ± 0.4
γ192−286	559 ± 25	
fibrinogen[c]	21 ± 3	4.4 ± 0.1

[a] Obtained by solid-phase binding assay. The values are means ± SD of three independent experiments. [b] Obtained by surface plasmon resonance. The values are means ± SD of two independent experiments. [c] The K_d values for fibrinogen were determined in similar experiments and are given for comparison.

Interaction between α_MI and the γ-Module Variants Detected by Solid-Phase Binding Assay. In solid-phase binding experiments, the γ-module and its fragments were immobilized onto plastic wells and increasing concentrations of the biotinylated α_MI-domain were added, followed by incubation and subsequent detection of the bound protein with streptavidin conjugated to alkaline phosphatase. A dose-dependent binding with different affinities was observed in all cases (Figure 4C). Binding of α_MI to the γ-module occurred with K_d of 22 nM; a similar K_d (21 nM) was obtained for the γ148−392 fragment (Table 1). At the same time, the NH_2- and COOH-terminal halves, γ148−286 and γ287−411, exhibited much weaker binding (K_d of 521 and 194 nM, respectively), in agreement with the ligand blotting data. These results indicate that the two halves contribute to the interaction between the γ-module and α_MI in a synergistic manner.

In another set of experiments, when the α_MI-domain was immobilized onto plastic wells and increasing concentrations of the γ-module and the same fragments were added followed by detection of the bound fragments with biotinylated polyclonal anti-γ-module antibodies as in ref *17*, no binding was observed (not shown). This suggested that either the α_MI-domain was inactivated upon adsorption onto plastic wells or the binding sites were cryptic in the soluble fragments. To further clarify the situation, we employed surface plasmon resonance (SPR) in which immobilization of proteins occurs through chemical cross-linking to a dextran matrix.

SPR-Detected Interaction between α_MI and the γ-Module Variants. In SPR experiments, the α_MI-domain was immobilized on a BIAcore CM-5 sensor chip surface and its interaction with the γ-module and its NH_2- and COOH-terminal halves, all added at 10 μM, was monitored in real time. None of the proteins exhibited binding (not shown). At the same time, in a control experiment, neutrophil inhibitory factor (NIF), a potent inhibitor of the $\alpha_M\beta_2$-fibrin(ogen) interactions (*4*, *18*), exhibited strong binding at 0.1 μM, suggesting that immobilized α_MI preserved at least some of its activities (not shown). Although these results are in agreement with the solid-phase binding experiments reinforcing the speculation that in solution the binding sites in the γ-module and its fragments are cryptic, one cannot exclude another explanation(s). Namely, since immobilization of α_MI occurs through chemical cross-linking, involvement in such cross-linking of residues that might be critical for the binding could inactivate α_MI. To reduce such possibility, we performed similar experiments with the α_MI-domain fused with GST-protein (GST-α_MI). As with the isolated α_MI, neither the γ-module nor its fragments added at the same 10 μM concentration exhibited binding to immobilized GST-α_MI (not shown). All these are in agreement with the idea that the $\alpha_M\beta_2$-binding sequences are cryptic in the nonimmobilized γ-module and its fragments.

In another set of SPR experiments, when α_MI was added to the immobilized γ-module and its recombinant halves, γ148−286 and γ287−411, a dose-dependent binding was observed (not shown). The K_d value for the binding to the γ-module was found to be 5.5 μM and those for the binding to γ148−286 and γ287−411 were 17.6 and 11.7 μM, respectively (Table 1). This result is in agreement with those obtained by ligand blotting and by solid-phase binding assay with the immobilized γ-module and its fragments, however, the affinities in this case were much lower for all three species. It should be noted that in control experiments the affinity of α_MI to immobilized fibrinogen determined by SPR (K_d = 21 nM) was also much lower that that determined by ELISA (K_d = 4.4 μM) (Table 1). The most probable explanation is that the chemical coupling of the fragments to a sensor chip surface perturbed their structure causing partial exposure of their $\alpha_M\beta_2$-binding sequences. However, such perturbation seems to be marginal in comparison with that caused by their adsorption onto plastic wells, resulting in much lower affinities.

Further Insight into the Binding Activity of the NH_2-Terminal Half of the γ-Module. Recent study demonstrated that the P2 sequence, but not P1, is the binding site for the α_MI-domain (*6*). Since the results described above indicated that both NH_2- and COOH-terminal halves of the γ-module bind α_MI well (the affinity of the former to α_MI is only 2-fold lower than that of the later), we further focused on the NH_2-terminal γ148−286 region to directly test the contribution of its P1 to the binding. This region consists of two independently folded domains formed by γ148−191 and γ192−286, respectively, the latter including the P1 sequence, γ190−202. We tested interaction of α_MI with the recombinant fragments, γ148−286, γ148−191, and γ192−286, corresponding to this region and its individual domains, and with the γ148−226 fragment including the NH_2-terminal domain and P1, by ligand blotting and solid-phase binding assay (Figure 5). Both methods revealed that among the fragments only γ148−286 and γ192−286 exhibited binding. This binding was dose-dependent, and the calculated K_d values were very similar, 521 and 559 nM (Table 1). This clearly indicated that the binding activity is located in the central domain of the γ148−286 fragment. Further, the fact that the γ148−226 fragment containing P1 sequence did not bind α_MI suggested that this sequence plays a marginal role in the interaction, in agreement with the previous report (*6*), and that additional sequence(s) in the central domain should possess $\alpha_M\beta_2$-binding activity.

Localization of the $\alpha_M\beta_2$-Binding Activity in the γ228−253 Region of the Central Domain of the γ-Module. To search for a putative $\alpha_M\beta_2$-binding sequence in the central domain of the γ-module, we digested the γ192−286 fragment with *o*-iodosobenzoic acid, which cleaves at tryptophan residues (*13*). Since this fragment has three potential cleavage sites, Trp^{208}−Ile^{209}, Trp^{227}−Leu^{228}, and Trp^{253}−Asn^{254}, we

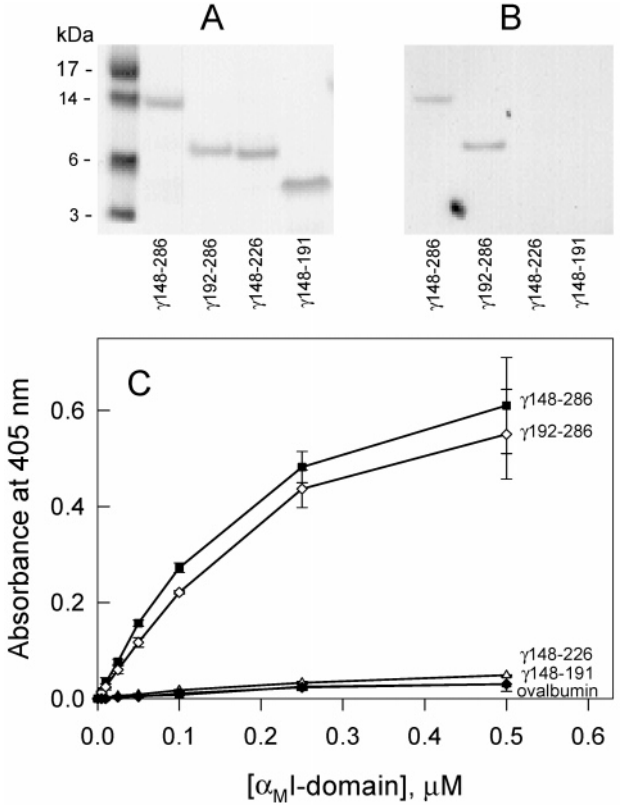

FIGURE 5: Analysis of binding of the α_MI-domain to the NH_2-terminal fragments of the γ-module by ligand blotting and solid-phase binding assay. The recombinant fragments γ148−286, γ192−286, γ148−226, and γ148−191 were transferred to the PVDF membrane after SDS−PAGE, stained with MemCode reversible protein stain kit (Pierce) (panel A), and then probed with biotinylated α_MI-domain after destaining (panel B). Panel C represents the results of the solid-phase binding assay. Increasing concentrations of the biotinylated α_MI-domain were incubated with microtiter wells coated with the indicated fragments and ovalbumin, which was used as a control. Bound α_MI-domain was detected using streptavidin conjugated to alkaline phosphatase. Error bars reflect the standard deviation of three independent determinations. All experiments were performed in TBS containing 1 mM $MnCl_2$. Solid lines represent the best fits of the data to eq 1, the corresponding values of K_d are presented in Table 1. Note that the curve for γ148−286 is essentially the same as that presented in Figure 4C.

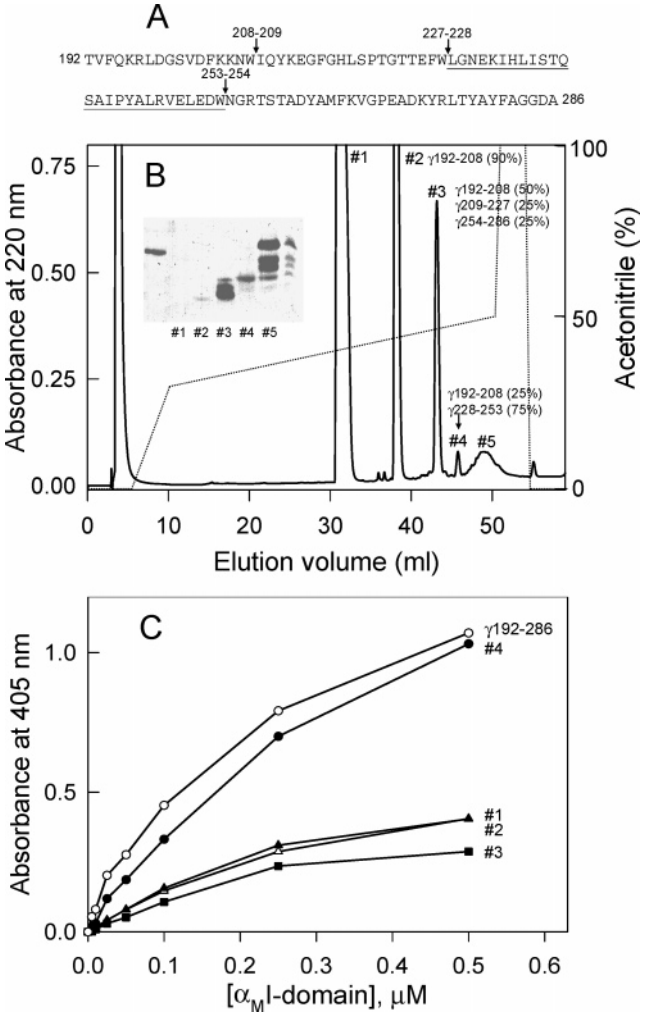

FIGURE 6: Fractionation and analysis of the chemical digest of the γ192−286 fragment. Panel A represents the amino acid sequence of the γ192−286 fragment. The arrows indicate the expected cleavage sites (see text), and the γ228−253 sequence is underlined. Panel B represents the HPLC profile of the *o*-iodosobenzoic acid digest of the γ192−286 fragment. The 30−50% gradient of acetonitrile was applied as shown by the dotted line. The inset in panel B shows SDS−PAGE analysis of individual fractions of the digest corresponding to the indicated peaks; the outer left line contains the intact γ192−286 fragment, while the outer right line contains its digest. The results of sequence analysis of each individual fraction are shown next to the peak number (see text). Panel C shows binding of the α_MI-domain to the individual fractions of the digest by solid-phase binding assay. Increasing concentrations of the biotinylated α_MI-domain were incubated with microtiter wells coated with the material from four peaks shown in panel B, the γ192−286 fragment was used as a control. Bound α_MI was detected using streptavidin conjugated to alkaline phosphatase. All experiments were performed in TBS containing 1 mM $MnCl_2$.

expected to obtain four subfragments, γ192−208, γ209−227, γ228−253, and γ254−286 (Figure 6A). When the cleaved material was fractionated by HPLC, five peaks were observed (Figure 6B). These were analyzed by SDS−PAGE and sequenced. SDS−PAGE analysis revealed no protein material in the first fraction (peak 1), a low molecular mass fragment in the second fraction (peak 2), a mixture of three low molecular mass fragments in the third fraction (peak 3), two fragments with an intermediate mobility in the fourth fraction (peak 4), and a number of fragments including the noncleaved parent γ192−286 in the fifth peak (Figure 6B, inset). Sequence analysis confirmed that peak 1 did not contain protein and revealed that peak 2 contained 90% pure γ191−208 subfragment, peak 3 contained three subfragments, γ192−208 (∼50%), γ209−227 (∼25%) and γ254−286 (∼25%), and peak 4 contained mostly the γ228−253 sub-fragment (∼75%) and small amount (∼25%) of the γ191−208 subfragment. The fraction from peak 5 containing the noncleaved γ192−286 fragment was not sequenced. Thus, all expected cleavage products were recovered from the γ192−286 digest.

We next tested the ability of each fraction to bind the biotinylated α_MI-domain by solid phase binding assay. Among the fractions analyzed, only that from the fourth peak containing the γ228−253 and γ192−208 subfragments exhibited substantial binding to α_MI (Figure 6C). This binding was comparable with that of the parent γ192−286 fragment. The other fractions exhibited much lower binding activity. In fact, since the material from the first peak, which according to the SDS−PAGE and sequence analysis did not contain protein, exhibited binding curve similar to those

obtained with the second and third peaks, all three curves reflect most probably nonspecific binding. These results suggested that the binding sequence is located within either the γ228−253 or γ192−208 subfragments, or both. However, since the γ148−226 fragment including γ192−208 exhibited practically no binding activity toward α_MI (Figure 5C), and since the second and third fractions containing respectively ~90 and ~50% of the γ192−208 subfragment were also inactive (Figure 6C), we concluded that the central domain of the γ-module contains a novel $\alpha_M\beta_2$-binding sequence within the γ228−253 region. This region is highlighted in yellow in the ribbon diagrams of the γ-module presented in Figure 1A.

DISCUSSION

The original goal of this study was to test whether separation of P1 and P2 in the γ-module by the hypothesized "pull out" mechanism (*9*, *10*) (see Figure 1A) could affect their relative contribution to the interaction of fibrin(ogen) with leukocyte integrin $\alpha_M\beta_2$ and thus would contribute to regulation of this interaction. For this purpose, we prepared recombinant fragments mimicking the arrangements of P1 and P2 in the intact structure and in the hypothetical γ-module with "pulled out" P2. They include the γ-module, containing both P1 and P2, and its NH_2- and COOH-terminal halves (fragments) containing either P1 or P2, respectively. Since the boundaries of the fragments, γ148−286 and γ287−411, were selected between the crystallographycally determined central and COOH-terminal domains (*8*), both were refolded into a compact structure as revealed by the fluorescence studies. The recombinant active form of the α_MI-domain including residues Glu123−Lys315 (*12*) was selected as a model of the fibrin(ogen)-binding region of $\alpha_M\beta_2$. The binding experiments revealed that the affinities of the fragments for α_MI were much lower than that of the γ-module, indicating that both halves of the latter are required for high affinity to occur. This suggests that the "pull out" of the P2 region from the central domain of the γ-module could result in a dramatic decrease of the affinity between fibrin(ogen) and $\alpha_M\beta_2$, in agreement with the hypothesis about a possible regulatory role of the "pull out" mechanism.

Another important finding of this study is that the central domain of the γ-module contains a novel $\alpha_M\beta_2$-binding sequence. The existence of an alternative (additional to P1 and P2) $\alpha_M\beta_2$-binding sequence(s) in the γ-module was predicted based on the finding that deletion from it of the γ383−411 segment including P2 resulted in only a 50% decrease of the α_MI-domain binding (*6*). In this study, we found that one of such sequences is located in the central domain of the γ-module and further localized it within the γ228−253 region. In the three-dimensional structure, this region forms an α-helix and β-strand (Figure 1A). Interestingly, this β-strand is located on the same surface as P1 and P2 and, in fact, forms with them an antiparallel three-stranded β-sheet. Whether the $\alpha_M\beta_2$-binding sequence is located in this β-strand, in the α helix, or in both, remains to be established.

The P1 sequence was originally implicated in the interaction with $\alpha_M\beta_2$ (*3*). In fact, the previous studies revealed that the synthetic γ190−202 peptide mimicking this sequence supported adhesion of the $\alpha_M\beta_2$-expressing cells and inhibited their adhesion to the immobilized fibrinogen fragments (*2*−*4*). It was found later that another sequence, γ377−395 or P2, was also involved in the binding and was more active than P1 (*4*, *20*). Further, when the γ196−199 residues in the P1 region of the P2-less γ-module were mutated, no effect on the binding activity of the latter was observed, resulting in the conclusion that the P2 sequence, but not P1, is the binding site for the α_MI-domain (*6*). At the same time, since these four residues are exposed in the three-dimensional structure of the γ-module (*8*, *21*), and since the $\alpha_M\beta_2$-binding site is cryptic in the latter (*7*), one could speculate that they are not involved in the interaction and that other residues of P1 are responsible. Therefore, this question needed further clarification. Our study clearly demonstrates that P1 in the γ148−226 fragment, in which it should be fully exposed, is not active. At the same time, this study does not rule out that the P1 sequence may possess some binding activity that was too low to be detected by the methods we used. In this respect, we did not observe any reasonable interaction of α_MI with the immobilized material from the second peak of the digest, which included the P1-containing γ192−208 subfragment (Figure 6). In addition, in a similar experiment synthetic P1 peptide also failed to bind α_MI (not shown). Thus, if P1 has any $\alpha_M\beta_2$-binding activity, it should be low in comparison with that of the other binding sequences of the γ-module.

Although a minimal recognition motif of the P2 sequence, P2-C, was localized to the γ390−395 residues, deletion of the γ391−411 segments from recombinant human fibrinogen did not change its ability to support adhesion of the $\alpha_M\beta_2$-expressing HEK 293 cells (*6*). It was also found that deletion of this segment from the recombinant γ-module decreased the amount of the α_MI-domain bound to the mutant by only about 26% (*6*). In agreement, this study revealed that the affinity to α_MI of the γ-module variant, γ148−392, in which three out of five residues of the motif were deleted, was practically the same as that of the full-length γ-module (Table 1). All these observations indicate that the γ390−395 motif contributes only marginally to the interaction when it is a part of the γ-module or fibrinogen structure. At the same time, it was shown recently that mutant mouse fibrinogen, in which the γ390−396 segments were converted to a series of alanine residues, failed to support adhesion of various mouse and human cell lines including HEK 293 (*22*). The explanation for such a dramatic difference in the results obtained with human (*6*) and mouse (*22*) mutant fibrinogens is not obvious. One can only speculate that it could be attributed to different mechanisms of interaction of fibrinogen with $\alpha_M\beta_2$ in these two species. Further studies are required to interpret these conflicting observations.

In our experiments, none of the tested fragments interacted with the immobilized α_MI-domain either in solid-phase binding assay or in SPR, in agreement with the cryptic character of the $\alpha_M\beta_2$-binding site in soluble fibrinogen reported recently (*7*, *22*, *23*). The fragments exhibited α_MI-binding activity only when they were immobilized. In solid phase binding assays, in which the fragments were immobilized by adsorption onto plastic, they exhibited high affinity; in SPR experiments, in which the fragments were immobilized to a dextran-coated surface by chemical cross-linking, their affinities were much lower (Table 1). These suggest that chemical immobilization perturbed their con-

formations only moderately in comparison with adsorption onto a surface and that the $\alpha_M\beta_2$-binding sites are fully exposed only in the adsorbed fragments. This is in agreement with previous reports indicating that surface-adsorbed fibrinogen has altered conformation (*24*−*27*). Thus, the high-affinity interaction between the α_MI-domain of $\alpha_M\beta_2$ and the γ-module of fibrinogen observed in this study occurs only when the latter is adsorbed. Such interactions could be physiologically important in vivo for quick inflammatory response to exposure of the damaged vasculature and tissues to foreign surfaces. It may also trigger undesirable inflammation upon contact of fibrinogen with implanted biomaterials (*23*, *28*, *29*). It should be noted that fibrinogen undergoes conformational changes also upon conversion into fibrin (*30*) and that association of fibrinogen/fibrin with the extracellular matrix resulted in unmasking of the P2-C motif of P2 (*7*). The question of whether such changes result in the exposure and activity of other $\alpha_M\beta_2$-binding sequences and the overall affinity of fibrin to $\alpha_M\beta_2$ remains to be clarified.

In summary, in this study we performed quantitative analysis of the interaction between fibrinogen and leukocyte integrin $\alpha_M\beta_2$ using their recombinant binding domains and combinations thereof, the γ-module fragments and the α_MI-domain, respectively. The analysis revealed that α_MI interacts with the γ-module with high affinity, that both the central domain of the γ-module and its P2-containing COOH-terminal half are required for high affinity to occur, and that separation of P2 from the central domain may contribute to regulation of this interaction. Such high-affinity interaction was observed only with the surface-adsorbed γ-module, in agreement with the cryptic character of the $\alpha_M\beta_2$-binding site in fibrinogen. We also identified a novel $\alpha_M\beta_2$-binding sequence in the central domain of the γ-module and further localized this sequence within its γ228−253 region. This sequence, together with P2 and other recently identified α_MI-binding sequences (*31*) seem to form a complex $\alpha_M\beta_2$-binding site whose activity depends on availability/exposure of its composing elements.

ACKNOWLEDGMENT

We thank Dr. I. Pechik for help in preparation of the ribbon diagrams of the γ-module.

REFERENCES

1. Altieri, D. C., Agbanyo, F. R., Plescia, J., Ginsberg, M. H., Edgington, T. S., and Plow, E. F. (1990) A unique recognition site mediates the interaction of fibrinogen with the leukocyte integrin Mac-1 (CD11b/CD18), *J. Biol. Chem. 265*, 12119−12122.
2. Medved, L., Litvinovich, S., Ugarova, T., Matsuka, Y., and Ingham, K. (1997) Domain structure and functional activity of the recombinant human fibrinogen γ-module (γ148−411), *Biochemistry 36*, 4685−4693.
3. Altieri, D. C., Plescia, J., and Plow, E. F. (1993) The structural motif glycine 190-valine 202 of the fibrinogen γ chain interacts with CD11b/CD18 integrin ($\alpha_M\beta_2$, Mac-1) and promotes leukocyte adhesion, *J. Biol. Chem. 268*, 1847−1853.
4. Ugarova, T. P., Solovjov, D. A., Zhang, L., Loukinov, D. I., Yee, V. C., Medved, L. V., and Plow, E. F. (1998) Identification of a novel recognition sequence for integrin $\alpha_M\beta_2$ within the γ-chain of fibrinogen, *J. Biol. Chem. 273*, 22519−22527.
5. Yalamanchili, P., Lu, C., Oxvig, C., and Springer, T. A. (2000) Folding and function of I domain-deleted Mac-1 and lymphocyte function-associated antigen-1, *J. Biol. Chem. 275*, 21877−21882.
6. Ugarova, T. P., Lishko, V. K., Podolnikova, N. P., Okumura, N., Merkulov, S. M., Yakubenko, V. P., Yee, V. C., Lord, S. T., and Haas, T. A. (2003) Sequence γ377−395(P2), but not γ190−202(P1), is the binding site for the α_MI-domain of integrin $\alpha_M\beta_2$ in the γC-domain of fibrinogen, *Biochemistry 42*, 9365−9373.
7. Lishko, V. K., Kudryk, B., Yakubenko, V. P., Yee, V. C., and Ugarova, T. P. (2002) Regulated unmasking of the cryptic binding site for integrin $\alpha_M\beta_2$ in the γC-domain of fibrinogen, *Biochemistry 41*, 12942−12951.
8. Yee, V. C., Pratt, K. P., Cote, H. C. F., Le Trong, I., Chung, D. W., Davie, E. W., Stenkamp, R. E., and Teller, D. C. (1997) Crystal structure of a 30 kDa C-terminal fragment from the γ chain of human fibrinogen, *Structure 5*, 125−138.
9. Yakovlev, S., Litvinovich, S., Loukinov, D., and Medved, L. (2000) Role of the β-strand insert in the central domain of the fibrinogen γ-module, *Biochemistry 39*, 15721−15729.
10. Yakovlev, S, Loukinov, D., and Medved, L. (2001) Structural and functional role of the β-strand insert (γ381−390) in the fibrinogen γ-module. A "pull out" hypothesis, *Ann. N. Y. Acad. Sci. 936*, 122−124.
11. Muchowski, P. J., Zhang, L., Chang, E. R., Soule, H. R., Plow, E. F., and Moyle, M. (1994) Functional interaction between the integrin antagonist neutrophil inhibitory factor and the I domain of CD11b/CD18, *J. Biol. Chem. 269*, 26419−26423.
12. Xiong, J. P., Li, R., Essafi, M., Stehle, T., and Arnaout, M. A. (2000) An isoleucine-based allosteric switch controls affinity and shape shifting in integrin CD11b A-domain, *J. Biol. Chem. 275*, 38762−38767.
13. Burgess, R. R., Arthur, T. M., and Pietz, B. C. (2000) Mapping protein−protein interaction domains using ordered fragment ladder far-western analysis of hexahistidine-tagged fusion proteins, *Methods Enzymol. 328*, 141−157.
14. Gill, S. C., and von Hippel, P. H. (1989) Calculation of protein extinction coefficients from amino acid sequence data, *Anal. Biochem. 182*, 319−326.
15. Lishko, V. K., Yakubenko, V. P., and Ugarova, T. P. (2003) The interplay between integrins $\alpha_M\beta_2$ and $\alpha_5\beta_1$ during cell migration to fibronectin, *Exp. Cell Res. 283*, 116−126.
16. Lishko, V. K., Yakubenko, V. P., Hertzberg, K. M., Grieninger, G., and Ugarova, T. P. (2001) The alternatively spliced α_EC domain of human fibrinogen-420 is a novel ligand for leukocyte integrins $\alpha_M\beta_2$ and $\alpha_X\beta_2$, *Blood 98*, 2448−2455.
17. Yakovlev, S., Makogonenko, E., Kurochkina, N., Nieuwenhuizen, W., Ingham, K., and Medved, L. (2000) Conversion of fibrinogen to fibrin: mechanism of exposure of tPA- and plasminogen-binding sites, *Biochemistry 39*, 15730−15741.
18. Zhang, L., and Plow, E. F. (1996) Overlapping, but not identical, sites are involved in the recognition of C3bi, neutrophil inhibitory factor, and adhesive ligands by the $\alpha_M\beta_2$ integrin, *J. Biol. Chem. 271*, 18211−18216.
19. Yokoyama, K., Zhang, X. P., Medved, L., and Takada, Y. (1999) Specific binding of integrin $\alpha_V\beta_3$ to the fibrinogen γ and α_E chain C-terminal domains, *Biochemistry 38*, 5872−5877.
20. Ugarova, T. P., and Yakubenko, V. P. (2001) Recognition of fibrinogen by leukocyte integrins, *Ann. N. Y. Acad. Sci. 936*, 368−385.
21. Spraggon, G., Everse, S. J., and Doolittle, R. F. (1997) Crystal structures of fragment D from human fibrinogen and its crosslinked counterpart from fibrin, *Nature* 389, 455−462.
22. Flick, M. J., Du, X., Witte, D. P., Jirouskova, M., Soloviev, D. A., Busuttil, S. J., Plow, E. F., and Degen, J. L. (2004) Leukocyte engagement of fibrin(ogen) via the integrin receptor $\alpha_M\beta_2$/Mac-1 is critical for host inflammatory response in vivo, *J. Clin. Invest. 113*, 1596−1606.
23. Hu, W. J., Eaton, J. W., Ugarova, T. P., and Tang, L. (2001) Molecular basis of biomaterial-mediated foreign body reactions, *Blood 98*, 1231−1238.
24. Procyk, R., Kudryk, B., Callender, S., and Blomback, B. (1991) Accessibility of epitopes on fibrin clots and fibrinogen gels, *Blood 77*, 1469−1475.
25. Zamarron, C., Ginsberg, M. H., and Plow, E. F. (1991) A receptor-induced binding site in fibrinogen elicited by its interaction with platelet membrane glycoprotein IIb-IIIa, *J. Biol. Chem. 266*, 16193−16199.
26. Ugarova, T. P., Budzynski, A. Z., Shattil, S. J., Ruggeri, Z. M., Ginsberg, M. H., and Plow, E. F. (1993) Conformational changes in fibrinogen elicited by its interaction with platelet membrane glycoprotein GPIIb-IIIa, *J. Biol. Chem. 268*, 21080−21087.

27. Moskowitz, K. A., Kudryk, B., and Coller, B. S. (1998) Fibrinogen coating density affects the conformation of immobilized fibrinogen: implications for platelet adhesion and spreading, *Thromb. Haemostasis 79*, 824−831.
28. Tang, L., and Eaton, J. W. (1993) Fibrin(ogen) mediates acute inflammatory responses to biomaterials, *J. Exp. Med. 178*, 2147−2156.
29. Tang, L., Ugarova, T. P., Plow, E. F., and Eaton, J. W. (1996) Molecular determinants of acute inflammatory responses to biomaterials, *J. Clin. Invest. 97*, 1329−1334.
30. Medved, L., Tsurupa, G., and Yakovlev, S. (2001) Conformational changes upon conversion of fibrinogen into fibrin. The mechanisms of exposure of cryptic sites, *Ann. N. Y. Acad. Sci. 936*, 185−204.
31. Lishko, V. K., Podolnikova, N. P., Yakubenko, V. P., Yakovlev, S., Medved, L., Yadav, S. P., and Ugarova, T. P. (2004) Multiple binding sites in fibrinogen for integrin $\alpha_M\beta_2$ (Mac-1), *J. Biol. Chem. 279*, 44897−44906.

BI048266W